Journal of Physiology (1990), **431**, *pp.* 291–318
With 14 *figures*
Printed in Great Britain

PROPERTIES OF A HYPERPOLARIZATION-ACTIVATED CATION CURRENT AND ITS ROLE IN RHYTHMIC OSCILLATION IN THALAMIC RELAY NEURONES

BY DAVID A. MCCORMICK* AND HANS-CHRISTIAN PAPE†

*From the *Section of Neuroanatomy, Yale University School of Medicine, 333 Cedar Street, New Haven, CT 06510, USA and †Abt. Neurophysiologie, Medizinische Fakultaet, Ruhr-Universitaet, D-4630 Bochum, FRG*

(*Received 3 April 1990*)

SUMMARY

1. The physiological and functional features of time-dependent anomalous rectification activated by hyperpolarization and the current which underlies it, I_h, were examined in guinea-pig and cat thalamocortical relay neurones using *in vitro* intracellular recording techniques in thalamic slices.

2. Hyperpolarization of the membrane from rest with a constant-current pulse resulted in time-dependent rectification, expressed as a depolarizing sag of the membrane potential back towards rest. Under voltage clamp conditions, hyperpolarizing steps to membrane potentials negative to approximately −60 mV were associated with the activation of a slow inward current, I_h, which showed no inactivation with time.

3. The activation curve of the conductance underlying I_h was obtained through analysis of tail currents and ranged from −60 to −90 mV, with half-activation occurring at −75 mV. The time course of activation of I_h was well fitted by a single-exponential function and was strongly voltage dependent, with time constants ranging from greater than 1–2 s at threshold to an average of 229 ms at −95 mV. The time course of de-activation was also described by a single-exponential function, was voltage dependent, and the time constant ranged from an average of 1000 ms at −80 mV to 347 ms at −55 mV.

4. Raising $[K^+]_o$ from 2·5 to 7·5 mM enhanced, while decreasing $[Na^+]_o$ from 153 to 26 mM reduced, the amplitude of I_h. In addition, reduction of $[Na^+]_o$ slowed the rate of I_h activation. These results indicate that I_h is carried by both Na^+ and K^+ ions, which is consistent with the extrapolated reversal potential of −43 mV. Replacement of Cl^- in the bathing medium with isethionate shifted the chloride equilibrium potential positive by approximately 30–70 mV, evoked an inward shift of the holding current at −50 mV, and resulted in a marked reduction of instantaneous currents as well as I_h, suggesting a non-specific blocking action of impermeable anions.

5. Local (2–10 mM in micropipette) or bath (1–2 mM) applications of Cs^+ abolished I_h over the whole voltage range tested (−60 to −110 mV), with no consistent effects on instantaneous currents. Barium (1 mM, local; 0·3–0·5 mM, bath) evoked a steady

* Author for correspondence.

inward current, reduced the amplitude of instantaneous currents, and had only weak suppressive effects on I_h.

6. Block of I_h with local application of Cs^+ resulted in a hyperpolarization of the membrane from the resting level, a decrease in apparent membrane conductance, and a block of the slow after-hyperpolarization that appears upon termination of depolarizing membrane responses, indicating that I_h contributes substantially to the resting and active membrane properties of thalamocortical relay neurones.

7. A sub-population of cat dorsal lateral geniculate nucleus neurones generated rhythmic high-frequency bursts of action potentials with an interburst frequency of 1–2 Hz. Intracellular recordings indicate that this activity results from the interaction of the low-threshold Ca^{2+} current I_t with the hyperpolarization-activated cation current I_h. It is proposed that the presence and physiological characteristics of I_h contribute substantially to the physiological properties of thalamic neurones during periods of inattentiveness and slow-wave sleep.

INTRODUCTION

Thalamocortical relay neurones possess two basic modes of action potential generation which vary according to the state of the animal: (1) single-spike firing occurs during attentiveness and waking and (2) rhythmic burst firing occurs during periods of inattentiveness and sleep (Steriade & Deschênes, 1984; Steriade & Llinás, 1988). Intracellular investigations both *in vivo* and *in vitro* have revealed that these two modes of action potential generation depend upon both the intrinsic electrophysiological properties of thalamic neurones and the interconnections of the different subtypes of thalamic cells, especially between the γ-aminobutyric acid-containing neurones of the nucleus reticularis and the neurones located in individual relay nuclei (Jahnsen & Llinás, 1984*a*, *b*; Steriade & Deschênes, 1984; Steriade & Llinás, 1988). One of the prominent features of thalamic relay neurones is that upon hyperpolarization of the membrane there appears strong time-dependent inward rectification which moves the membrane potential back towards the normal resting value (Crunelli, Kelly, Leresche & Pirchio, 1987*a*; McCormick & Pape, 1988; Lightowler, Hynd, Pollard & Crunelli, 1989). Since the membrane potential of thalamic relay neurones that are rhythmically oscillating *in vivo* continuously fluctuates within the voltage range in which this rectification is present (Steriade & Deschênes, 1984), the underlying current may be of importance for shaping the electrical behaviour of these neurones, although its ionic basis and voltage dependence have not yet been characterized.

In many different types of electrically responsive cells, including heart cells, and neurones in the sensory and sympathetic ganglia, spinal cord, brain stem, cerebellum, hippocampus and cerebral cortex, hyperpolarization of the membrane results in a depolarizing sag back towards rest (Hotson, Prince & Schwartzkroin, 1979; Halliwell & Adams, 1982; Mayer & Westbrook, 1983; DiFrancesco, 1985; Crepel & Penit-Soria, 1986; Spain, Schwindt & Crill, 1987; Bobker & Williams, 1989; Eng, Gordon, Kocsis & Waxman, 1990; Tokimasa & Akasu, 1990). The current underlying this phenomenon is carried by both Na^+ and K^+ ions, activates upon membrane hyperpolarization (typically beyond -60 mV), and de-activates upon depolarization. In sino-atrial cells and Purkinje fibres of the heart, this type of current,

termed I_f, appears to be important in determining the rate of action potential generation (Noble, DiFrancesco & Denyer, 1989). In the central nervous system, in contrast, the role of hyperpolarization-activated cation currents is less clear. Potential roles in determining the resting membrane potential and modulating the response to hyperpolarizing inputs have been suggested (Halliwell & Adams, 1982; Spain *et al.* 1987). An additional possibility is that I_h contributes to rhythmic cellular oscillations (Alonso & Llinás, 1989). In particular, the recent demonstration of endogenous oscillations in thalamocortical relay neurones maintained *in vitro* at membrane potentials in which time-dependent anomalous rectification is prevalent (Haby, Leresche, Jassik-Gerschenfeld, Soltesz & Crunelli, 1988; McCormick & Prince, 1988) suggests a possible important contribution of I_h to this type of electrophysiological behaviour.

Here we describe some of the physiological characteristics of the current which underlies this form of anomalous rectification and investigate its contribution to the electrophysiological behaviour of thalamocortical relay cells.

METHODS

Thalamic slices were prepared from male or female guinea-pigs (200–300 g) or cats (four; approximately 2·5 kg) as described previously (Crunelli, Leresche, Hynd, Patel & Parnavelas, 1987*b*; McCormick & Pape, 1988; McCormick & Prince, 1988). The animals were deeply anaesthetized (pentobarbitone, 40 mg/kg I.P., guinea-pigs; ketamine, 25 mg/kg I.M., followed by pentobarbitone, 36 mg/kg I.V., cats) and killed by decapitation. A block of tissue containing the dorsolateral aspect of the thalamus was removed and placed in physiological saline at a temperature of 5 °C. Slices were prepared as 400 μm thick coronal sections on a Vibratome (Ted Pella, Model 1000) and placed in an interface-type recording chamber (Fine Science Tools). Slices were maintained at 36 ± 1 °C and continuously superfused with a solution containing (in mM): NaCl, 126; KCl, 2·5; $MgSO_4$, 1·2–2; $NaHCO_3$, 26; NaH_2PO_4, 1·25; $CaCl_2$, 2; dextrose, 10; saturated with 95% O_2, 5% CO_2 to a final pH of 7·4. Recording commenced 2 h after preparation of the slices.

Intracellular recordings were obtained with thin-wall micropipettes (World Precision Instruments, TW-100), prepared on a micropipette puller (Flaming–Brown, P-80/PC) and filled with 4 M-potassium acetate. Final resistances ranged between 35 and 55 MΩ.

An Axoclamp 2A amplifier (Axon Instruments) was used for both current and voltage clamp recordings. During current clamp recordings, the bridge balance was continuously monitored. During single-electrode voltage clamp, head stage output was continuously monitored to ensure adequate settling time. Sampling frequencies were between 3·5 and 5·5 kHz and the amplifier gain was typically around 1 nA/mV. Voltage clamp experiments were performed using the pClamp software program (Axon Instruments) operating on an IBM AT computer. The degree of 'space clamp' obtained in these neurones under our conditions is unknown. However, the finding that the rate and voltage dependence of activation of I_h were both well behaved, in that they were smooth and continuous functions of the membrane potential, suggests that sufficient clamp was obtained in order to avoid serious errors. Data were digitized (Neurocorder DR-384) and stored on magnetic tape with a video cassette recorder for later analysis or collected on-line with the computer. Only neurones having stable membrane potentials negative to −55 mV, resting input resistances above 30 MΩ and action potentials which overshot 0 mV were included for analysis. In the cat dorsal lateral geniculate nucleus, recordings were obtained from neurones located in the A-laminae.

Changing the ionic composition of the bathing medium was achieved by the following equimolar substitutions: (a) extracellular sodium concentration was decreased by replacing NaCl with choline chloride; (b) extracellular potassium concentration was increased by substitution of KCl for NaCl; and (c) extracellular chloride concentration was reduced by replacing NaCl by sodium isethionate, and KCl by potassium acetate. DC offsets due to changes in junction potential at the Ag–AgCl reference electrode in different chloride concentrations were compensated in the following way: the membrane potential at which single-spike firing was elicited was determined in normal bathing

solution. During introduction of a different chloride solution, this firing threshold was repeatedly monitored and its reading was kept constant by adding current to the input offset circuitry of the amplifier. Complete exchange, indicated by a constant reference potential, was typically achieved in 30–60 min. At the end of the experiment, the change in reference potential was controlled by measuring the DC offset of the electrode in normal bathing solution. Finally, when Mn^{2+} or Ba^{2+} were added to the superfusate, $MgCl_2$ was substituted for $MgSO_4$ and NaH_2PO_4 was removed to avoid precipitation.

Caesium and barium were applied to thalamic neurones either in the bathing medium (Cs^+, 1–2 mM; Ba^{2+}, 500 μM) or locally to the exposed surface of the slice with a broken micropipette (Cs^+, 2–20 mM; Ba^{2+}, 1 mM). Drug-applying micropipettes had a tip diameter of approximately 2–5 μm and substances were extruded in volumes of 5–15 pl by applying a brief pressure pulse of nitrogen (10–20 ms, 207–345 kPa) to the pipette. In some experiments, Ni^{2+} (1 mM), 4-aminopyridine (4-AP, 0·5–1 mM), tetraethylammonium (10 mM) or tetrodotoxin (TTX, 0·2 μM) were introduced in the perfusion medium. Averaged data are represented as mean ± standard deviation.

RESULTS

The data presented here are based largely upon recordings obtained from neurones in the guinea-pig dorsal lateral geniculate nucleus (LGND; $n = 67$). Additional recordings from cells in the LGND of the cat ($n = 14$), as well as from the medial geniculate nucleus ($n = 9$) of both species, revealed similar results and therefore were combined for analysis. A representative sample of twenty guinea-pig LGND neurones possessed a resting membrane potential of -66 ± 3 mV, apparent input resistance of 46 ± 12 MΩ and spike amplitude of 91 ± 6 mV. All neurones reported here exhibited large rebound burst discharges upon repolarization of the membrane after a brief hyperpolarization, strong inward rectification when hyperpolarized, and delayed onset to firing when depolarized. These electrophysiological properties suggest that these neurones were thalamocortical relay neurones (Jahnsen & Llinás, 1984*a*, *b*; McCormick & Pape, 1988) and therefore we refer to them as such.

Hyperpolarization of thalamic relay neurones beyond approximately −60 mV resulted in a slowly activating rectification, apparent as a depolarizing sag of the membrane potential back towards the normal resting value (Fig. 1*A*, arrows). Both the amplitude of this rectification and the apparent rate of its activation increased markedly with incremental increases in the hyperpolarizing current pulse (Fig. 1*A*). In neurones located in other parts of the nervous system, termination of a hyperpolarizing current pulse is often associated with the generation of a rebound depolarizing potential, resulting in part from the slow de-activation of the current underlying anomalous rectification (Mayer & Westbrook, 1983; Spain *et al.* 1987). In thalamic relay cells, the membrane potential changes upon termination of a hyperpolarizing response are complicated by the interacting effects of de-activation of anomalous rectification with activation of other currents, such as the low-threshold calcium current (Jahnsen & Llinás, 1984*a*, *b*; Coulter, Huguenard & Prince, 1989; Crunelli, Lightowler & Pollard, 1989; Hernández-Cruz & Pape, 1989) and transient potassium currents (Jahnsen & Llinás, 1984*a*, *b*; D. A. McCormick, unpublished observations).

In single-electrode voltage clamp, hyperpolarizing voltage steps from a holding potential of −55 mV resulted in a slow inward relaxation, the time course and amplitude of which was dependent on the amplitude of the voltage step (Fig. 1*B*, arrows). The injection of short duration conductance test pulses (50 ms duration, 10 mV amplitude) during the development of this inward relaxation revealed a

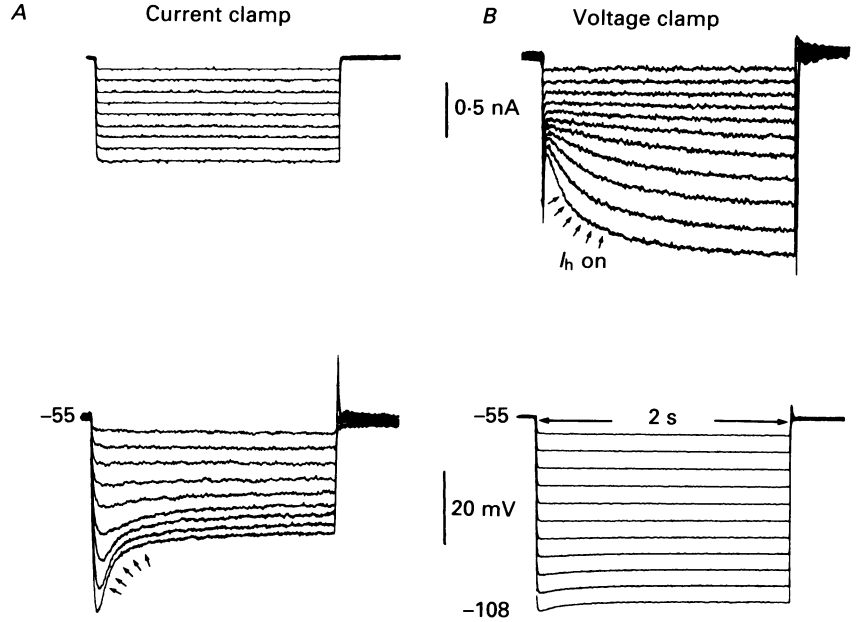

Fig. 1. Rectification of hyperpolarizing responses evoked in a guinea-pig LGND relay cell. Upper traces are membrane current; lower traces are membrane potential. Recordings are from the same cell, depolarized to −55 mV. *A*, in current clamp conditions hyperpolarizing current pulses (duration 1·9 s) evoke membrane hyperpolarizations that show a voltage- and time-dependent depolarizing 'sag' (arrows). *B*, under voltage clamp conditions, hyperpolarizing voltage steps elicit a slow inward current (I_h, arrows) whose amplitude and rate of activation increase with increasing hyperpolarization.

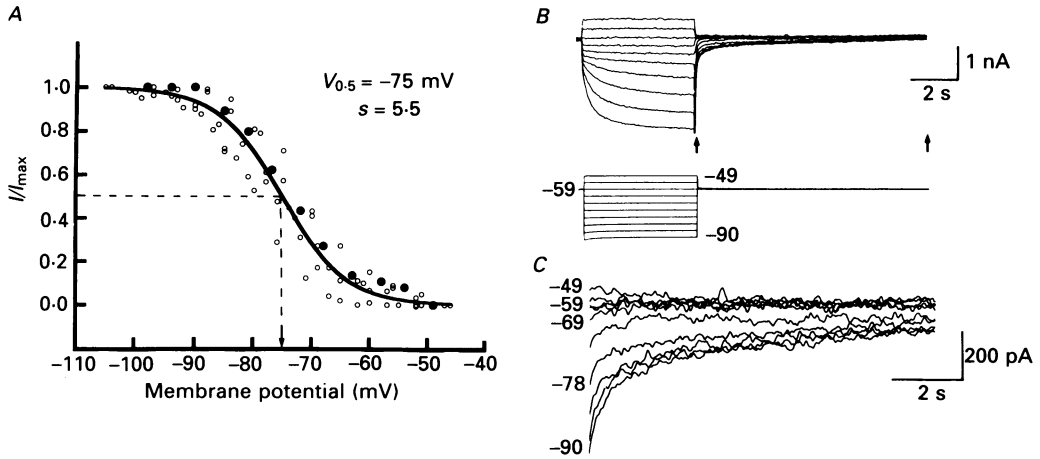

Fig. 2. Activation curve of the conductance, G_h, which underlies I_h. *A*, plot of the activation curve for G_h for seven different LGND relay neurones. Filled circles represent data obtained from cell illustrated in *B* and *C*. Line represents best fit using eqn (1) for data illustrated. *B*, incremental increases in hyperpolarizing steps from −40 to −90 mV progressively increase the amount of I_h which is activated. Tail currents between arrows are expanded for detail in *C*. Care was taken in measuring tail currents so as to minimize the contribution of capacitative or non-I_h active currents by allowing sufficient time for these events to dissipate before measuring I_h. See text for details.

substantial increase in membrane conductance (mean = 19·6 ± 5·7 nS; $n = 5$; −55 to −95 mV), indicating that it represented the activation of an inward current, rather than de-activation of an outward current.

In the following we will refer to this slow inward current as I_h because it is activated by hyperpolarization. In agreement with the results in current clamp, the amplitude of I_h increased markedly with increases in the size of the hyperpolarizing voltage step (Fig. 1*B*). The threshold for activation of I_h appeared to be approximately −60 to −65 mV and at −95 mV the amplitude of I_h ranged from 0·5 to 2·0 nA (e.g. Figs 1–3). The current did not decay during voltage steps longer than 1 min in duration, indicating very little, if any, inactivation of the conductance underlying I_h.

Activation curve

The activation curve of the membrane conductance underlying I_h (G_h) was constructed by measuring tail currents elicited by repolarizing the membrane to holding level (typically −60 mV) following voltage steps of 4–5 s to between −55 and −105 mV (Fig. 2). This experimental protocol was chosen to reduce contamination of I_h tail currents by other currents, the possible contribution of which was further minimized in some neurones by including Ni^{2+} (1 mM) to block low-threshold calcium currents (Coulter *et al.* 1989; Crunelli *et al.* 1989; Hernández-Cruz & Pape, 1989), 4-aminopyridine (0·5–1 mM) to block transient potassium outward currents (such as I_A and I_D, Storm, 1988), and tetrodotoxin (TTX, 0·2 μM) to block transient and persistent voltage-gated sodium currents and spontaneous synaptic potentials. The tail current amplitudes were normalized to the maximal amplitude and plotted against the membrane potential to which the neurone was stepped during activation of I_h. The resulting data were well fitted by the Boltzmann equation:

$$I/I_{max} = (1 + \exp((V_m - V_{0.5})/s))^{-1}, \quad (1)$$

were V_m is the membrane potential, $V_{0.5}$ is the membrane potential at which G_h is half-activated, I is the amplitude of the tail current at the beginning of I_h de-activation and s is the slope factor which determines the steepness of the fitted curve (e.g. Mayer & Westbrook, 1983; Hagiwara & Irisawa, 1989).

In this manner, the activation range of G_h was between −60 and −95 mV, with half-activation occurring at an average of −74·6 ± 3·4 mV ($n = 7$) with a slope factor (s) of 5·5 ± 0·8 (Fig. 2*A*).

Time course of activation and de-activation

The rate of activation of I_h increased markedly as the membrane potential was hyperpolarized (Figs 1*B* and 3). Over the whole voltage range tested, I_h was well

Fig. 3. Time constants of I_h activation and de-activation. *A*, plot of the voltage dependence of I_h activation and de-activation as calculated from the data presented in *B–E*. Progressive hyperpolarizing voltage steps activate I_h (*B*). The current traces during the 3 s interval indicated are expanded in *D* in which the data are fitted with a single-exponential function (circles represent actual data; line is best fit). Voltage dependence of I_h de-activation was examined by fully activating I_h and then stepping to membrane potentials between −83 and −55 mV (*C*). The current traces during the 3 s interval indicated were fitted with a single-exponential function (*E*). Data obtained after block of transient outward current with 4-aminopyridine and voltage-activated Na^+ currents with tetrodotoxin.

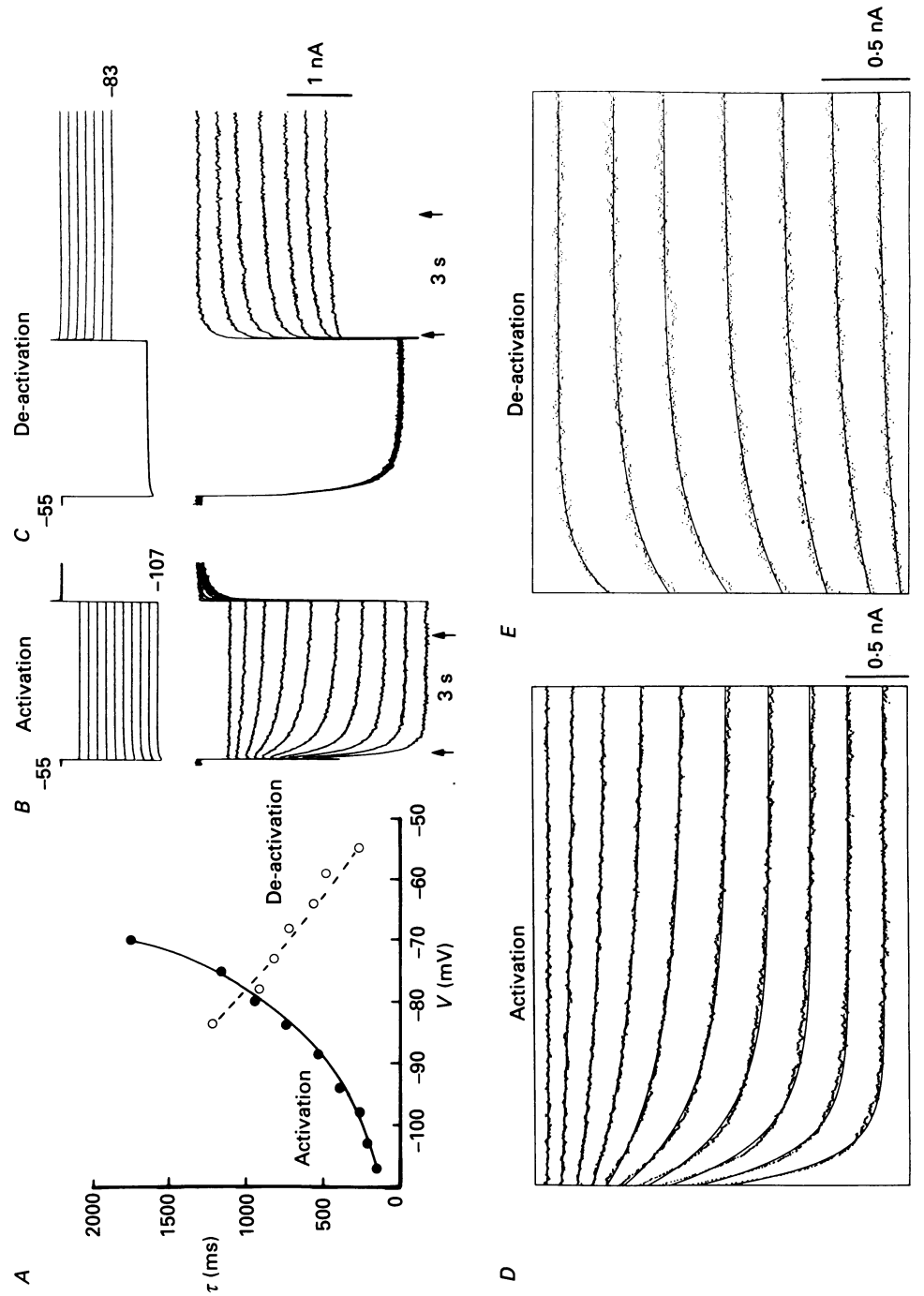

Fig. 3. For legend see facing page.

fitted ($r > 0.98$) by a single-exponential function of the form:

$$I_t = A_0 + A_1 e^{-t/\tau}, \quad (2)$$

where I_t is the amplitude of the current at time t, A_0 and A_1 are constants and τ is the time constant (Fig. 3*D*). τ ranged from greater than 1–2 s at membrane potentials just past threshold (e.g. −65 to −70 mV) to an average of 229 ms (±57 ms; $n = 7$) at −95 to −100 mV (Fig. 3*A*).

The rate of de-activation of I_h was determined through examining tail currents associated with depolarization of the membrane from a hyperpolarized level (e.g. −105 mV) or through envelope analysis. When examining tail currents, the transient outward potassium currents were typically blocked with local application of 4-aminopyridine (1–2 mM; $n = 5$) after block of synaptic transmission with local application of tetrodotoxin (10 μM). The amplitude and time course of I_h during de-activation was well fitted ($r > 0.95$) by a single-exponential function (Fig. 3*E*). The rate of de-activation of I_h was strongly voltage dependent (Fig. 3*A*) ranging from > 1 s at approximately −85 mV to an average of 347 ms (±97; $n = 5$) at −55 mV. The latter value of de-activation of I_h was confirmed through the use of envelope analysis (Mayer & Westbrook, 1983; Tokimasa & Akasu, 1990). In this protocol, the membrane potential was held at −95 mV for a sufficient time to fully activate I_h (e.g. 5 s) and was then transiently depolarized to between −60 and −55 mV for a varying length of time. The membrane was then repolarized to −95 mV and the amplitude of I_h activated by this repolarization was measured. Due to the lack of inactivation of I_h, this amplitude corresponds to the amount of I_h which de-activated during the transient depolarization. Using this experimental protocol, we determined the rate of de-activation of I_h to average 426±121 ms ($n = 6$) at −60 to −55 mV, a value which is in good agreement with the time constants obtained through analysis of tail currents.

Ionic composition of I_h

The nature of the ions carrying I_h through the membrane was investigated by changing the extracellular concentration of K^+, Na^+ and Cl^-. Raising the extracellular K^+ concentration ($[K^+]_o$) from 2·5 to 7·5 mM resulted in an inward current, an increase in membrane conductance, and an enhancement of I_h, as measured by the difference between the steady-state and instantaneous *I–V* relations (Fig. 4*A* and *B*; $n = 4$). Possible contamination of the steady-state currents by the K^+-carried inward rectifier, which at physiological intracellular magnesium concentrations is activated by hyperpolarization beyond the potassium equilibrium potential, E_K (Matsuda, Saigusa & Irisawa, 1987; Ishihara, Mitsuiye, Noma & Takano, 1989), can be assumed to be small, since the range of hyperpolarizing voltage pulses was largely positive to E_K (presumably −105 and −73 mV in 2·5 and 7·5 mM $[K^+]_o$, respectively; McCormick & Prince, 1987). These data indicate that a significant portion of I_h is carried by K^+.

Decreasing $[Na^+]_o$ from 153 to 26 mM resulted in a marked reduction of the amplitude of the hyperpolarization-activated steady-state current and a slower time course of activation at a given voltage (Fig. 5*A*; $n = 6$). In addition, the de-activating currents, emerging as tail currents after stepping back to the holding

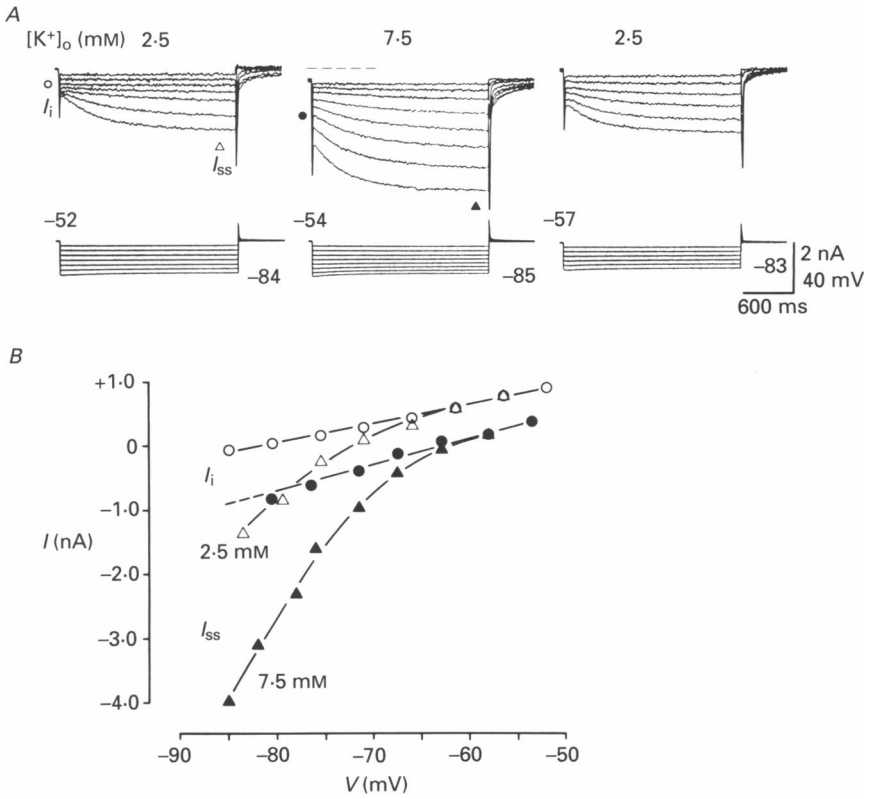

Fig. 4. Effects of changing the extracellular concentration of potassium ions, $[K^+]_o$, upon hyperpolarization-activated currents. *A*, family of currents (upper traces) evoked in a LGND neurone by hyperpolarizing voltage steps (lower traces) in control solution (2·5 mM $[K^+]_o$, left), during increased $[K^+]_o$ (7·5 mM, middle; dashed line for comparison in baseline holding current), and during recovery to control $[K^+]_o$ (2·5 mM, right). Holding potential and most negative steady-state step potential are indicated near traces; step amplitude is 5 mV, step duration is 2 s. *B*, *I–V* relationship for instantaneous currents (I_i, circles) and steady-state currents after 2 s (I_{ss}, triangles) obtained from experiment in *A*. Open symbols indicate control condition; filled symbols indicate elevated $[K^+]_o$. I_i at larger hyperpolarizations extrapolated (dashed line) from instantaneous *I–V* relationships at smaller hyperpolarizations, that were directly determined from measurement of current traces. Tail currents are contaminated by transient Ca^{2+} and K^+ currents. Note increased slope of the steady-state *I–V* relation during increased $[K^+]_o$ that exceeds increase in slope of the instantaneous *I–V* relationship.

potential of −50 mV, changed from small inward to clear outward currents in the low-Na^+ solution, indicating a negative shift of the reversal potential. Current *versus* voltage (*I–V*) relationships revealed a negative shift of the steady-state *I–V* relation in low Na^+, and no significant change in instantaneous current (Fig. 5*C*). These results indicate that Na^+ ions also contribute to I_h.

A possible contribution of Cl^- to I_h was examined by decreasing $[Cl^-]_o$ from 132·5 to 4 mM using isethionate. The low-Cl^- solution shifted E_{Cl}, which normally is approximately −75 mV, by up to 70 mV more positive, as indicated by the reversal potential of the muscimol- (0·1 mM, local application) induced chloride current. If a

large anion conductance contributed to I_h, this positive shift of E_{Cl} is expected to increase I_h in size. However, the low-Cl^- solution resulted in a substantial decrease in size of both the steady-state currents and the instantaneous currents activated by hyperpolarizing voltage steps, and in addition elicited an inward shift of the holding

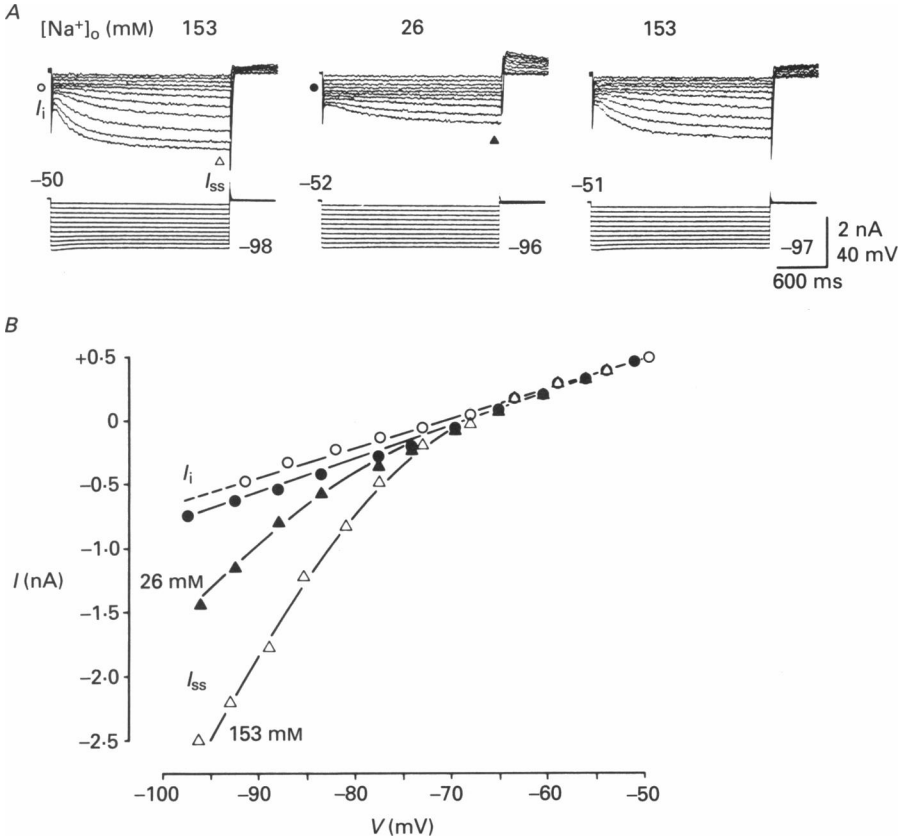

Fig. 5. Effects of changing the extracellular concentration of sodium ions, $[Na^+]_o$, upon I_h. *A*, family of currents (upper traces) evoked by hyperpolarizing voltage steps (lower traces) in control solution (153 mM $[Na^+]_o$, left), during reduced $[Na^+]_o$ (26 mM, middle), and during recovery to control $[Na^+]_o$ (153 mM, right). Pulse protocol as in Fig. 4. Note the reduced size and time course of activation in the steady-state currents, and the change in polarity of the de-activating tail currents in the low-Na^+ solution. *B*, *I–V* relationship obtained from data in *A*, with instantaneous currents (I_i) plotted as circles and steady-state currents (I_{ss}) plotted as triangles; open symbols represent control conditions and filled symbols reduced $[Na^+]_o$. Recordings in the same LGND neurone.

current at a potential of −50 mV (Fig. 6*A* and *B*; $n = 3$). Thus, the amplitude of I_h was significantly reduced in the low-Cl^- solution, suggesting a blocking action of isethionate ions on I_h. Interestingly, the time course of activation of I_h appeared unchanged during substitution of $[Cl^-]_o$. Similar blocking effects of impermeable anion substitutes on anomalous rectifier currents have been reported in sino-atrial node cells (Yanagihara & Irisawa, 1980) and sensory ganglion neurones (Mayer & Westbrook, 1983).

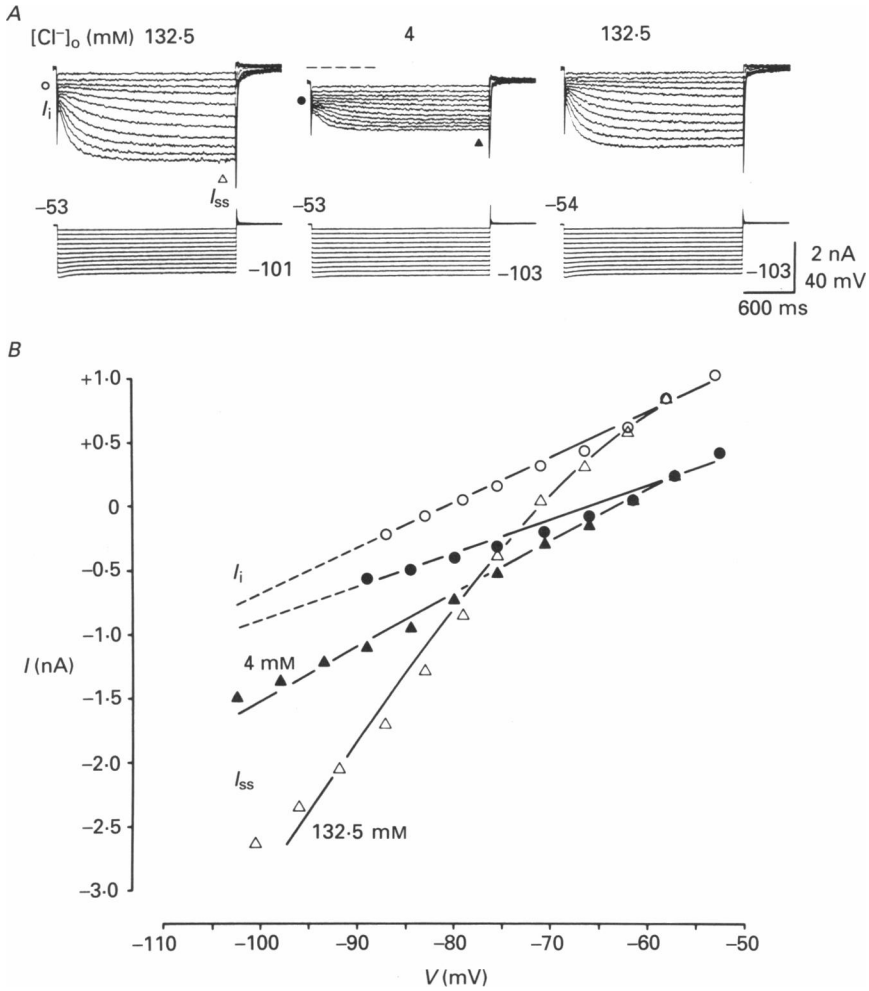

Fig. 6. Effects of changing the extracellular concentration of chloride ions, $[Cl^-]_o$, upon I_h. *A*, family of currents (upper traces) elicited by hyperpolarizing voltage commands (lower traces) in a single LGND neurone in control solution (132·5 mM $[Cl^-]_o$, left), during substitution of chloride ions by isethionate ions (4 mM $[Cl^-]_o$, middle; dashed line for comparison in baseline holding current), and during recovery in control solution (right). Pulse protocol as in Fig. 4. *B*, *I–V* relationship from experiment in *A*. Open symbols, control; filled symbols, reduced $[Cl^-]_o$. Low-Cl^- solution substantially reduces I_h, i.e. the difference between instantaneous currents (I_i) and steady-state currents (I_{ss}).

We conclude that both Na^+ and K^+ ions carry the hyperpolarization-activated current, I_h, in thalamic neurones, and suggest that Cl^- ions do not contribute substantially to this inwardly rectifying process.

Sensitivity of I_h to extracellular Cs^+ and Ba^{2+}

In many different cell types low concentrations of extracellular caesium ions (Cs^+), but not barium ions (Ba^{2+}), selectively block hyperpolarization-activated cation currents (Halliwell & Adams, 1982; Mayer & Westbrook, 1983; DiFrancesco, 1985;

Spain *et al.* 1987). In thalamocortical neurones, local (2–10 mM) or bath (1–2 mM) application of Cs^+ resulted in a selective reduction of I_h (Fig. 7*A* and *B*; $n = 12$). In contrast, Cs^+ appeared to have no consistent effect on the instantaneous components of the current responses (Fig. 7*A* and *B*).

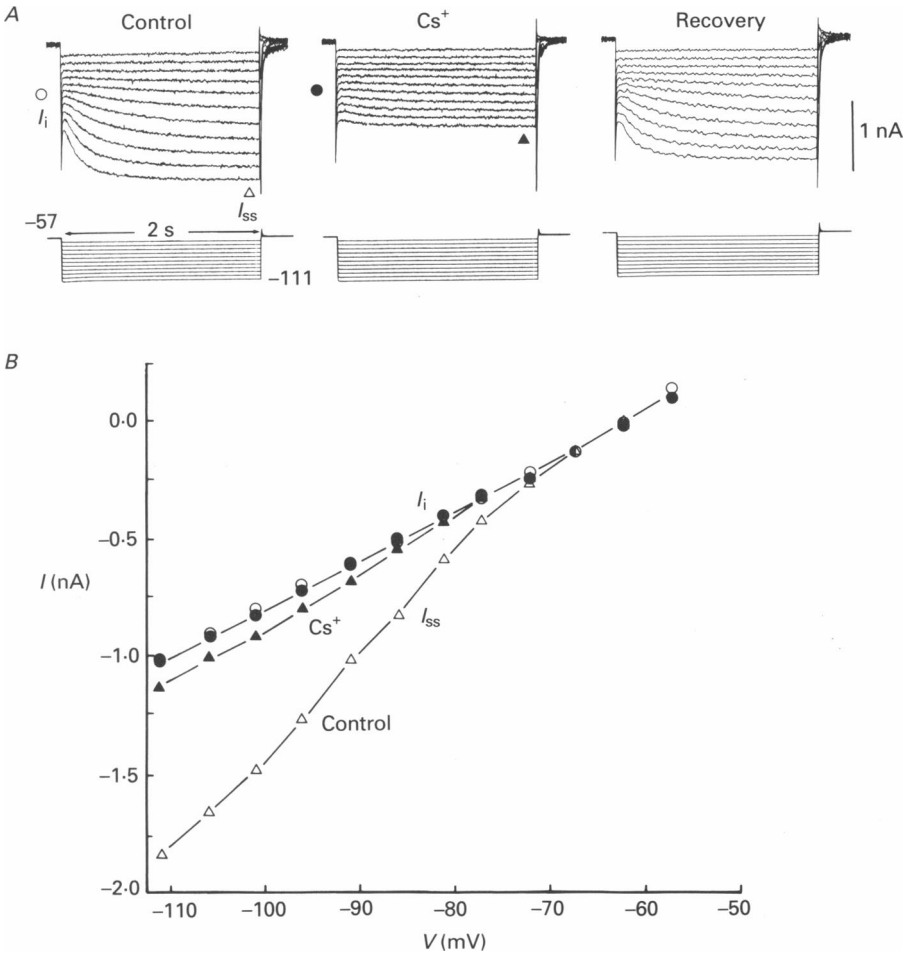

Fig. 7. Extracellular caesium blocks I_h. *A*, family of currents (upper traces) evoked by hyperpolarizing voltage steps (lower traces) under control conditions (left), after local application of caesium (Cs^+, 10 mM in micropipette; middle), and after recovery from Cs^+ (right). Holding potential and most negative step potential are indicated near traces; step amplitude is 5 mV; step duration is 2 s. *B*, *I–V* relationship obtained from experiment in *A*. Instantaneous current (I_i) is plotted as circles; steady-state current (I_{ss}) after 2 s is plotted as triangles. Open symbols represent currents under control condition; filled symbols are currents after application of Cs^+. Cs^+ blocks the time- and voltage-dependent inward current with no effect on instantaneous current.

In current clamp recordings, local or bath applications of Cs^+ resulted in a complete or near-complete block of the depolarizing 'sag' activated by hyperpolarization (e.g. Fig. 13*A*), confirming that this feature of electroresponsiveness is due to activation of I_h.

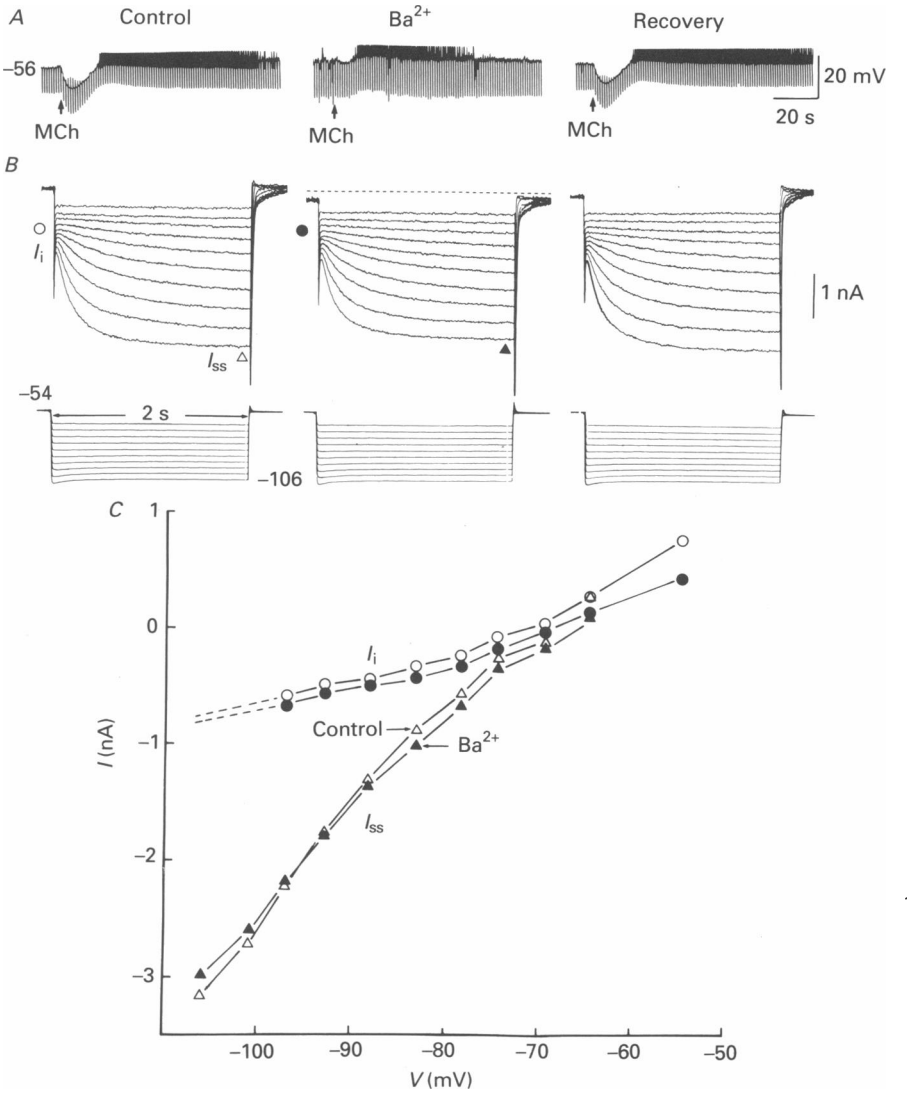

Fig. 8. Extracellular barium does not block I_h. *A*, hyperpolarizing–depolarizing response elicited by local application of the muscarinic-specific agonist acetyl-β-methylcholine (MCh, 5 mM), due to increase and decrease of membrane potassium conductances (McCormick & Prince, 1987). The hyperpolarizing response is reversibly antagonized by local application of Ba^{2+} (1 mM). *B*, same cell as in *A*. Inward currents (upper traces) elicited by stepping from a holding potential of −54 mV to −106 mV in increments of 5 mV (lower traces). Ba^{2+} evokes a small steady inward current (indicated by dashed line) and reduction in instantaneous current (I_i), but has very little, if any, effect on I_h (difference between I_{ss} and I_i). *C*, *I–V* relationship obtained from experiment in *B*. Open symbols represent control currents; filled symbols are currents during Ba^{2+}. Instantaneous current (I_i, circles) is slightly reduced by Ba^{2+}, whereas the steady-state current (I_{ss}, triangles) is relatively unaffected.

Extracellular application of Ba^{2+} either locally (1 mM) or in the bath (300–500 μM) to relay neurones held near firing threshold resulted in a small inward current, a reduction of instantaneous currents evoked by hyperpolarizing voltage pulses from about −50 mV, and only mild suppressive effects on I_h (Fig. 8*B* and *C*; $n = 4$).

In current clamp recordings, Ba^{2+} resulted in depolarization of the membrane, a decrease in apparent input conductance, and a potent and reversible block of the hyperpolarizing response elicited by the muscarinic agonist acetyl-β-methylcholine (5 mM, local application; Fig. 8*A*), known to be due to an increase in membrane potassium conductance (McCormick & Prince, 1987). In contrast, Ba^{2+} had no consistent effect on the depolarizing 'sag' activated by hyperpolarization (not shown).

Reversal potential

Determination of the reversal potential of I_h was achieved through two different methods. First, under voltage clamp conditions, the membrane potential was stepped from approximately −95 mV to potentials varying from −75 to −35 mV and the magnitude and polarity of the emerging tail currents during de-activation of I_h were measured. To minimize contamination of I_h tails by other currents, the cells were exposed to a number of channel blockers including Ni^{2+} (0·5 mM), 4-aminopyridine (0·5–1 mM), tetraethylammonium (10 mM), Ba^{2+} (1 mM) and tetrodotoxin (0·2 μM). In this manner, I_h tail currents reversed from inward to outward at approximately -43 ± 6 mV ($n = 3$).

To corroborate this reversal potential, a second method was used which takes advantage of the finding that I_h is selectively and potently blocked by local application of Cs^+ (see above). The neurone was voltage clamped well into the activation range of I_h (e.g. −90 mV) and voltage steps to varying potentials were applied (Fig. 9*A*). The instantaneous current at the beginning of each voltage step was determined, and a *I–V* relationship was constructed (Fig. 9*B*). Next, I_h was blocked through local application of Cs^+ (5–10 mM) and instantaneous *I–V* relationships were again determined. The extrapolated meeting point of the instantaneous *I–V* curves with and without contribution of I_h corresponds to the reversal potential of I_h. In this manner, the reversal potential was determined to be -43 ± 9 mV ($n = 8$), in agreement with the tail current analysis method above.

Functional properties of I_h

The ability of extracellular Cs^+ to selectively block I_h was used to investigate the contribution of I_h to the electrophysiological behaviour of thalamic neurones. Using this protocol, we have found I_h to contribute to three different electrophysiological characteristics of thalamic neurones: determination of the resting membrane potential, the occurrence of rhythmic burst firing, and the appearance of an after-hyperpolarization after removal of a depolarization.

Contribution of I_h to resting membrane potential

The resting membrane potential of thalamocortical relay neurones ranges from −62 to −75 mV which is within the activation range of I_h (see Fig. 2). Therefore, I_h may contribute significantly to the resting membrane properties of these neurones.

Indeed in current clamp recordings we found that local application of Cs^+ (5–20 mM; $n = 14$) while the cell was at rest resulted in a hyperpolarization of 5–10 mV (Figs 11–13) and a substantial increase in the amplitude of electrotonic responses induced by a hyperpolarizing current pulse (see Fig. 10*A* in McCormick & Pape, 1990).

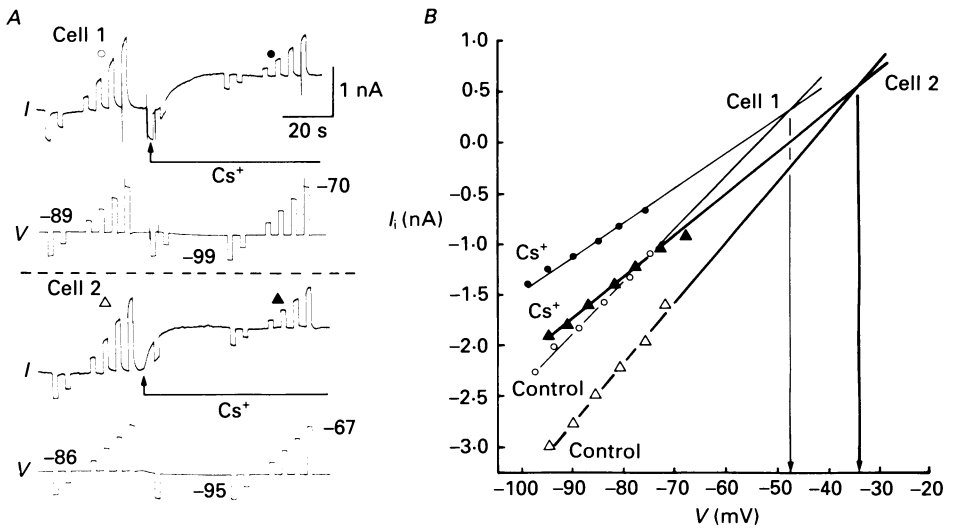

Fig. 9. Extrapolated reversal potential of I_h. *A*, inward and outward current relaxations (upper traces) upon hyperpolarizing and depolarizing voltage steps (lower traces) from two LGND cells, held at −89 mV (cell 1) and −86 mV (cell 2). Indicated near the voltage traces are the holding potential, the most positive and most negative step potentials. Step amplitude is 5 mV; step duration is 2 s. The slow inward and outward relaxations following the instantaneous currents represent activation and de-activation of I_h, respectively. Local application of caesium (Cs^+, 10 mM) results in a steady outward current and strongly reduced current relaxations, due to block of I_h. *B*, instantaneous *I–V* relationships obtained from the experiments shown in *A*. Cell 1 is plotted as circles, cell 2 as triangles. Open symbols represent instantaneous currents obtained under control conditions; filled symbols are instantaneous currents during Cs^+. Extrapolated intersection of instantaneous *I–V* curves with (control) and without (Cs^+) contribution of I_h occurs at the reversal potential of I_h. Curves fitted by eye. See text for further details.

In voltage clamp, these local applications of Cs^+ were associated with a selective and readily reversible reduction of I_h (see Fig. 7). These results indicate that I_h contributes substantially to determining the resting membrane potential of thalamocortical relay neurones.

Contribution of I_h to rhythmic burst firing

Extracellular recordings in cat LGND (but not guinea-pig LGND) revealed that a sub-population of thalamic relay neurones spontaneously and rhythmically generates high-frequency (300–500 Hz) bursts of two to six action potentials with an interburst frequency of 1–2 Hz (Haby *et al.* 1988; McCormick & Prince, 1988). Intracellular recordings from oscillating cat LGND neurones revealed that the slow 1–2 Hz oscillation is characterized by the regular occurrence of low-threshold Ca^{2+} spikes

(Fig. 10) which appear to be separated by an after-hyperpolarization (AHP). The oscillation was not dependent upon the occurrence of fast Na^+–K^+ action potentials, since at certain membrane potentials, the rhythmic low-threshold Ca^{2+} spikes were subthreshold for the generation of these fast spikes (not shown). Depolarization or

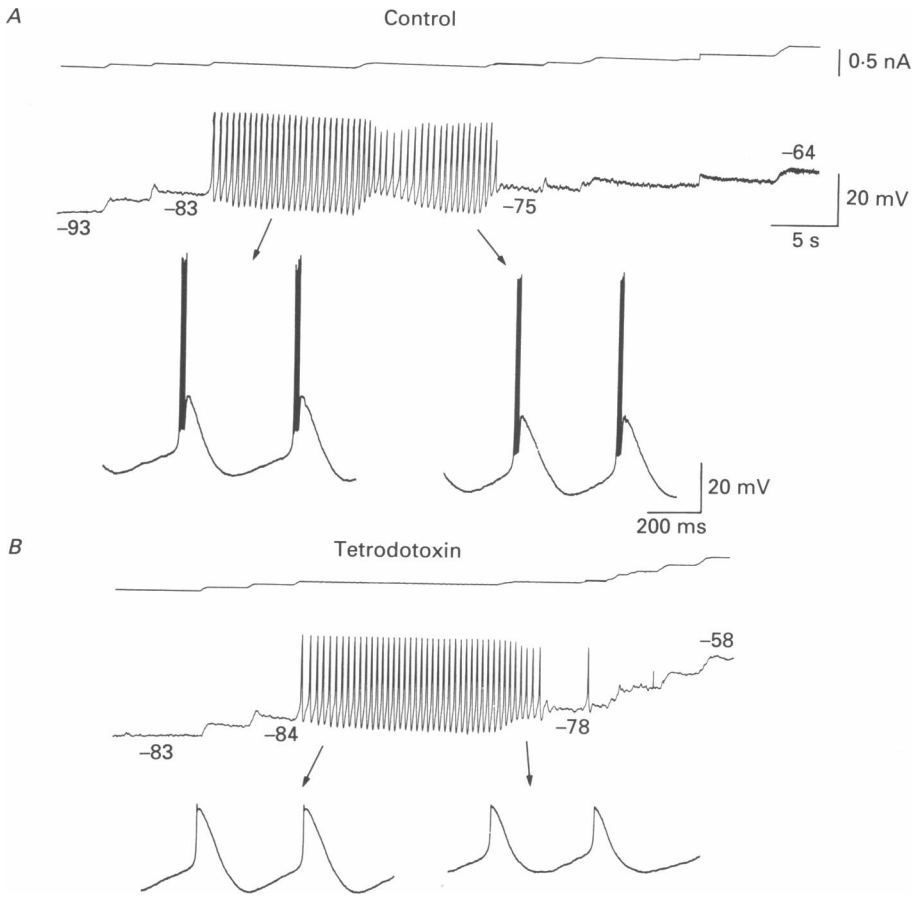

Fig. 10. Voltage dependence of 1–2 Hz oscillation in a cat LGND relay neurone. *A*, at membrane potentials between −93 and −83 mV, no oscillation or synaptic activity is seen. Slight depolarization of the neurone above −83 mV elicits a burst which is followed by rhythmic burst generation (see expanded traces). Further depolarization above approximately −75 mV abolishes rhythmic activity. *B*, local application of tetrodotoxin (10 μM) completely blocks fast action potentials and synaptic activity, but does not abolish rhythmic occurrence of low-threshold Ca^{2+} spikes. Both recordings from a cat LGND neurone.

hyperpolarization of the membrane through current injection revealed a small range of membrane potentials between approximately −85 and −70 mV at which this type of rhythmic activity can occur, and a relative lack of membrane or synaptic events which might be triggering the 1–2 Hz bursting. These data suggest that the rhythmic burst activity is an intrinsic property of the thalamocortical relay cell that

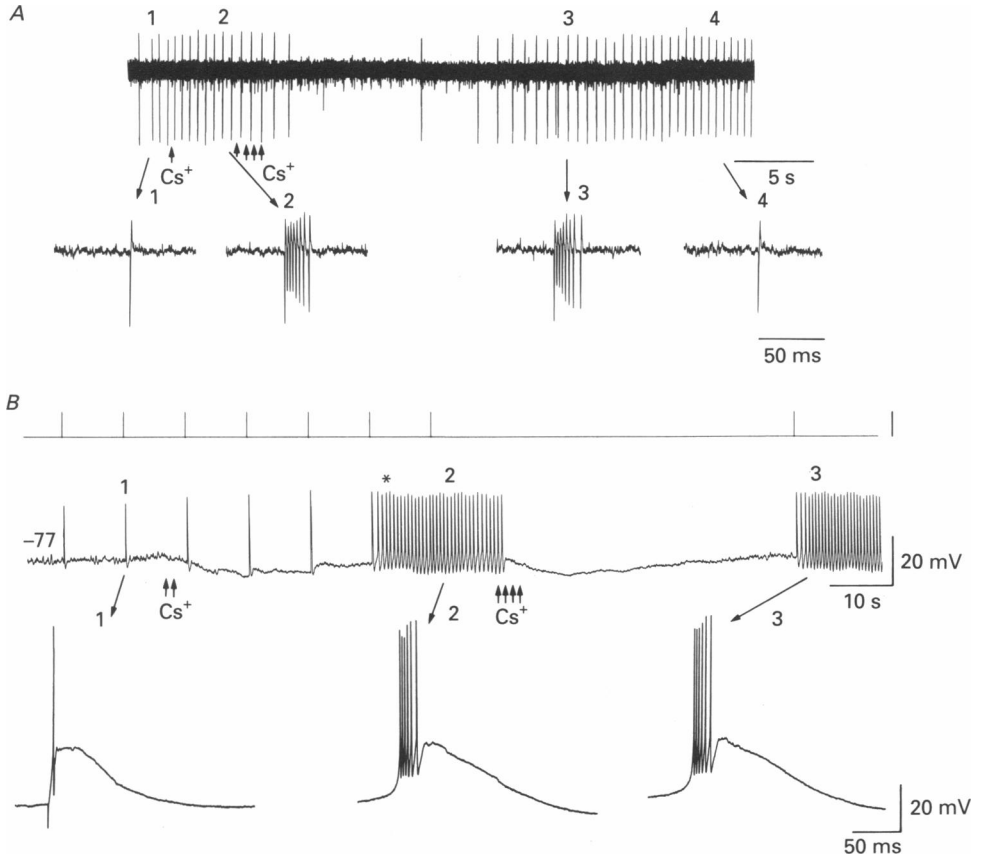

Fig. 11. Caesium enhances and blocks rhythmic burst firing in cat LGND neurones. *A*, extracellular recording of a spontaneously active LGND neurone. A single application of Cs^+ enhances rhythmic activity from the rhythmic generation of a single spike (*A*1) to rhythmic occurrence of bursts of eight action potentials (*A*2). Further applications of Cs^+ initially slows the rate at which bursts occur and finally abolishes all activity. Spontaneous activity slowly reappears with strong rhythmic bursts (*A*3) which gradually lessen back to single action potentials (*A*4). *B*, intracellular recording from a cat LGND neurone at −77 mV. Intracellular injection of a short duration (3 ms) depolarizing current pulse triggers a low-threshold Ca^{2+} spike and a single fast action potential, followed by a small AHP (*B*1). Application of Cs^+ results in a hyperpolarization and an enhancement of the burst, which now contains six fast action potentials. As the hyperpolarization lessens, rhythmic 1–2 Hz bursting activity can be triggered by the current pulse (asterisk). Further applications of Cs^+ can reversibly block this spontaneous activity.

can only occur at membrane potentials where both the low-threshold Ca^{2+} current is available for activation (Jahnsen & Llinás, 1984*a*, *b*) and I_h is prevalent. The endogenous nature of this activity was confirmed by the finding that local application of tetrodotoxin (10 μM) completely blocked fast action potentials and synaptic activity, but did not abolish the rhythmic oscillation (Fig. 10*B*). In addition, simultaneous extracellular recordings from two oscillating neurones with the same electrode revealed that each neurone exhibited its own particular frequency

of oscillation which was slightly different from that of its neighbour ($n = 6$). Thus, the oscillatory activity in the two cells slowly drifted into and out of phase, as would be expected by two independent oscillators (not shown).

The presence of rhythmic oscillation only at membrane potentials within the range of I_h activation suggests an important contribution of this current. This hypothesis

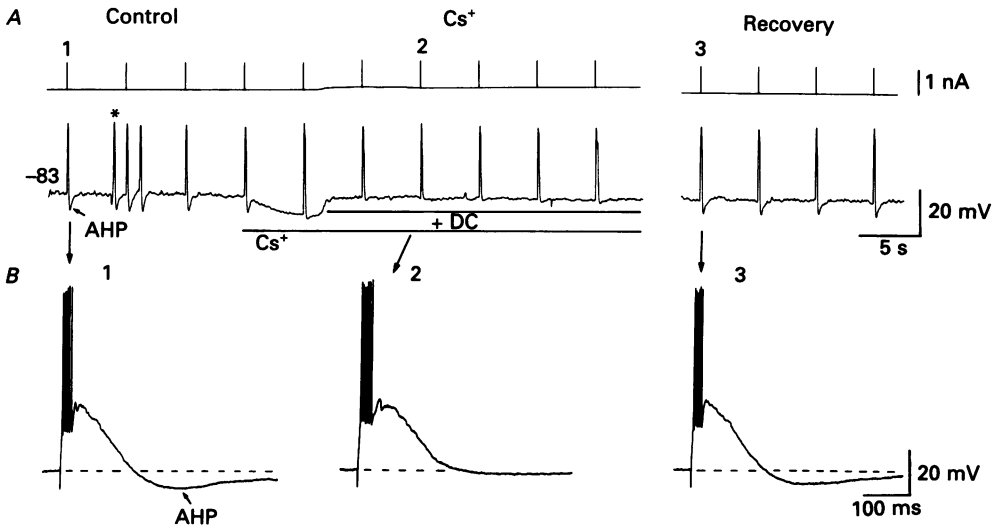

Fig. 12. Local application of Cs^+ blocks the burst after-hyperpolarization (AHP). *A*, intracellular injection of a short duration (3 ms) depolarizing current pulse into a cat LGND neurone at −83 mV results in a burst of six action potentials, followed by an AHP (*A*1 and *B*1), which can occasionally trigger rhythmic activity (asterisk). Local application of Cs^+ (10 mM) results in a hyperpolarization of the membrane potential and a reduction in the amplitude of the AHP. Compensation for the hyperpolarization with intracellular injection of current (+DC) reveals that the AHP is greatly reduced or abolished (*A*2 and *B*2). This effect is reversible (*A*3 and *B*3).

was tested through the selective block of I_h with local application of Cs^+ (5–10 mM). Interestingly, local application of Cs^+ to spontaneously oscillating neurones resulted in two effects, depending upon the dose administered. With small applications (e.g. one 10–15 pl microdrop placed on the surface of the slice within 50 μm of the entry point of the recording electrode), the rhythmic burst firing was markedly enhanced in that the number of spikes generated per burst was increased (Fig. 11, compare *A*1 and *A*2; $n = 11$). Further applications of Cs^+ resulted in further increases in the number of spikes per burst as well as a lengthening of the interburst interval which was generally followed by a complete and reversible cessation of activity (Fig. 11*A*). These results suggest that this pattern of rhythmic burst activity is strongly influenced by the presence and amplitude of I_h.

Intracellular recordings revealed that local application of small amounts of Cs^+ enhanced the probability of obtaining rhythmic burst firing ($n = 6$) while larger doses blocked this activity. For example, in the cell illustrated in Fig. 11*B*, injection of a short duration (3 ms) depolarizing current pulse activated a low-threshold Ca^{2+} spike and one fast action potential, but no oscillatory activity (Fig. 11*B*1). Local

application of Cs^+ resulted in hyperpolarization of the membrane. As this lessened 1–2 Hz rhythmic burst firing appeared, each phase of which was associated with a low-threshold Ca^{2+} spike which generated a burst of fast action potentials and a pronounced AHP (Fig. 11*B*2). Further applications of Cs^+ could disrupt this oscillation and replace it with a hyperpolarization. During repolarization, the rhythmic activity either spontaneously reappeared, or could be triggered by a single short depolarizing current pulse (Fig. 11*B*3).

These data suggest that the presence and characteristics of 1–2 Hz oscillation are strongly influenced by the presence and amplitude of I_h. One possible mechanism by which I_h may contribute to rhythmic burst firing is through the generation of a hyperpolarization following each burst. Indeed, generation of a single low-threshold Ca^{2+} spike was followed by the occurrence of a pronounced after-hyperpolarization (AHP; Fig. 12*A* and *B*), which could result in the occurrence of a brief period of rhythmic oscillation (Fig. 12*A*, asterisk). Application of small amounts of Cs^+ resulted in hyperpolarization of the membrane and a reduction in the AHP even though the burst response was enhanced. Compensation for the membrane hyperpolarization with intracellular injection of current revealed the burst AHP to be strongly reduced or abolished (Fig. 12*A*2 and *B*2). These results suggest that the burst AHP is generated by the de-activation of I_h during the burst and the subsequent activation of I_h after the burst. This hypothesis gives rise to a number of predictions. First, the AHP should not depend upon the occurrence of a low-threshold Ca^{2+} spike or fast action potentials, but rather should be present even after a passive depolarization. Second, the amplitude of the AHP should increase with increases in the duration of the depolarization. Third, the membrane conductance of the cell should increase as the AHP lessens, and fourth, the AHP should not occur at membrane potentials positive to the activation range of I_h.

All of these predictions were confirmed with intracellular recordings. Removal of a tonic depolarization which does not generate either a low-threshold Ca^{2+} spike or fast-action Na^+–K^+ action potentials is associated with the generation of an apparent slow AHP (Fig. 13*A* and *A*1). This apparent AHP increases in amplitude with increases in duration of the depolarization (Fig. 13*B*), and the rising phase of the AHP could activate a low-threshold Ca^{2+} spike (Fig. 13*B*). This ability of the slow AHP to activate a low-threshold Ca^{2+} spike only occurs at membrane potentials around -75 mV (Fig. 13*C*) and the slow AHP all but disappears if the neurone is tonically depolarized above -60 mV, even if a large number of action potentials are generated (Fig. 13*C*). In addition, injection of conductance test pulses during the generation of the slow AHP reveals that the membrane conductance is lowest at the peak of the hyperpolarization and slowly increases until the membrane potential once again stabilizes at the resting membrane potential (not shown). These properties suggest that this hyperpolarizing 'overshoot' is due to repolarization of the membrane through leakage channels which then shifts the membrane potential into a range in which I_h is active. Activation of I_h subsequently results in a steady depolarization which is both smooth and slow in time course. In this manner, the initial hyperpolarizing and subsequent depolarizing phase of the apparent after-hyperpolarization are due to a decreased and increased level of I_h activation, respectively.

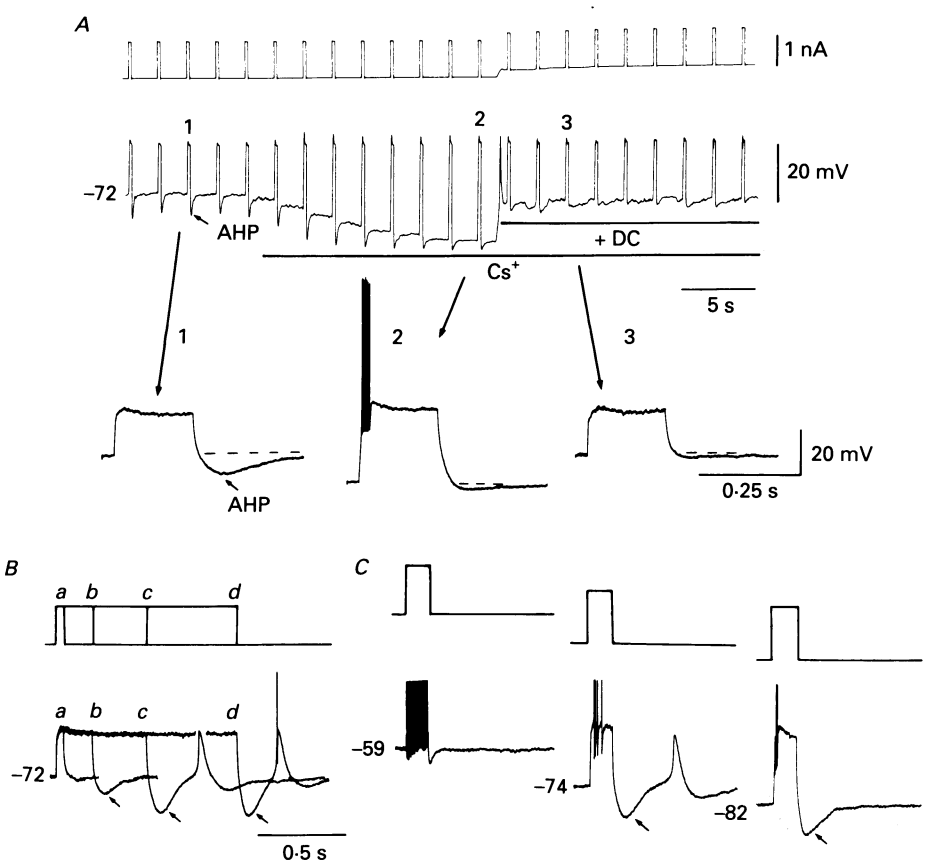

Fig. 13. Contribution of I_h to the resting potential and to the after-hyperpolarization (AHP). *A*, depolarization from normal resting potential (−72 mV) by intracellular injection of a current pulse, which does not result in a low-threshold Ca^{2+} spike or the generation of action potentials, is followed by a substantial after-hyperpolarization (trace expanded in *A*1). Local application of Cs^+ (20 mM in micropipette) results in a substantial hyperpolarization of the membrane, that de-inactivates the low-threshold Ca^{2+} spike, thereby activating a burst of fast action potentials (*A*2). Compensation for the hyperpolarization with the intracellular injection of current (+DC) reveals that the AHP is nearly abolished (compare *A*1 and *A*3). *B*, increasing the duration of the depolarizing current pulse results in a progressively larger AHP (arrows), that could generate a rebound low-threshold Ca^{2+} spike (*c* and *d*). *C*, voltage dependence of the AHP. A prolonged train of action potentials, elicited by a current pulse at −59 mV, is followed by only a short duration AHP. Hyperpolarization of the neurone to −74 mV results in the appearance of large AHP (arrow) even though the current pulse now causes only four action potentials. At this membrane potential, the AHP is associated with the generation of a rebound Ca^{2+} spike. Further hyperpolarization of the membrane to −82 mV abolishes the ability of the AHP to trigger a Ca^{2+} spike. All data collected from the same cat LGND layer A relay neurone. Spike amplitudes are truncated. Current calibration in *A* for *A*–*C*; voltage calibration in *A*3 to *A*1–*A*3, *B* and *C*. Time calibration in *B* for *B* and *C*.

These results indicate that I_h contributes substantially to the determination of the resting membrane potential, the generation of a slow after-hyperpolarization following a depolarization, and the occurrence of slow 1–2 Hz rhythmic burst firing (Fig. 14*B*). In this manner, thalamocortical relay cells display two firing modes. In

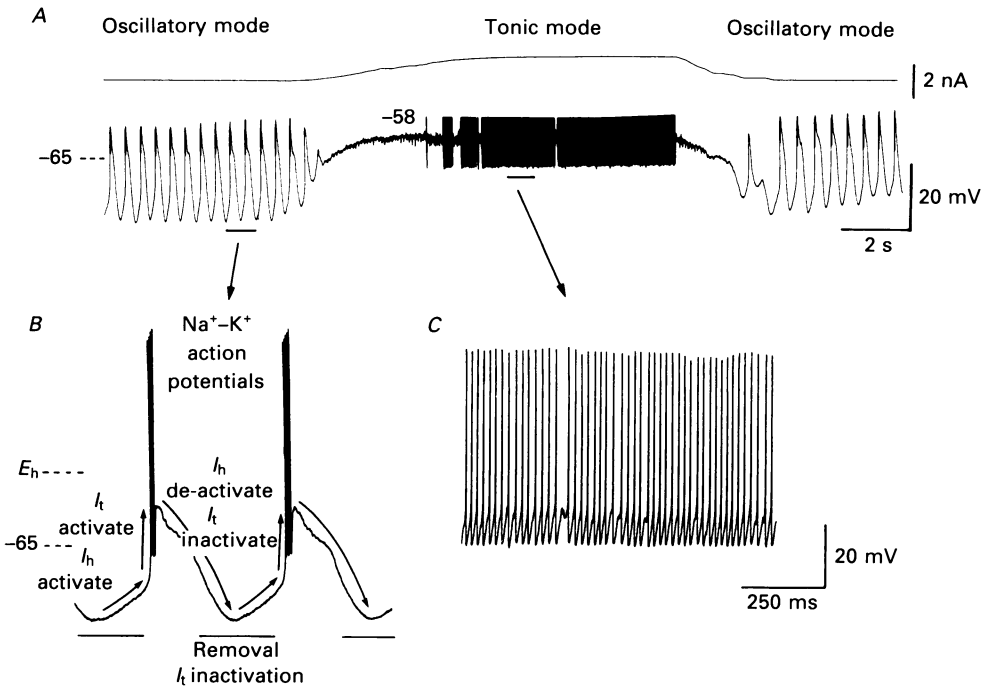

Fig. 14. Two different firing modes of thalamic relay neurones and the proposed ionic substrate of rhythmic burst firing. *A*, this cat LGND neurone generated rhythmic burst firing at a rate of about 2 Hz. Depolarization of the cell to −58 mV with the intracellular injection of current (top trace) halted the rhythmic activity and switched the neurone to the tonic, or single-spike, mode of action potential generation. Removal of the depolarization reinstated the oscillatory activity. *B*, expanded trace of oscillatory activity and the proposed currents which largely mediate it. Activation of the low-threshold calcium current, I_t, depolarizes the membrane towards threshold for a burst of Na^+- and K^+-dependent fast action potentials. The depolarization de-activates the portion of I_h that was active immediately before the Ca^{2+} spike. Repolarization of the membrane due to I_t inactivation is followed by a hyperpolarizing overshoot, due to the reduced depolarizing effect of I_h. The hyperpolarization in turn de-inactivates I_t and activates I_h, which depolarizes the membrane towards threshold for another Ca^{2+} spike. *C*, expanded trace of single-spike activity.

the lack of synaptic inputs, these neurones may exhibit endogenous rhythmic burst firing (Fig. 14*A*). We suggest that this rhythmic burst firing arises largely from the interaction of two dominant currents, I_t and I_h (see Discussion). Upon tonic depolarization of the membrane, as occurs for example during awakening from sleep (Hirsch, Fourment & Marc, 1983), this rhythmic activity is abolished by moving the membrane potential out of the range in which I_t and I_h are active (Fig. 14*A*), and switches the neurone to the tonic, or single-spike, mode of action potential generation (Fig. 14*C*), that allows faithful transfer of synaptic information (Steriade & Llinás, 1988).

DISCUSSION

Inward rectification in thalamic neurones

The present results demonstrate that thalamocortical relay neurones respond to hyperpolarization of the membrane with a time- and voltage-dependent inward rectification. The characteristics of the current, I_h, which underlies this rectification include permeability to both Na^+ and K^+ ions, a reversal potential (−43 mV) substantially positive to normal resting potential, and a sensitivity to extracellular Cs^+. The exact contribution of Cl^- to I_h in thalamic neurones remains to be delineated.

Hyperpolarization-activated ionic conductances are a prevalent feature of electrically excitable cells, including frog skeletal muscle fibres, heart, photoreceptors, neurones in the peripheral and central nervous system, and some types of axons (Halliwell & Adams, 1982; Mayer & Westbrook, 1983; DiFrancesco, 1985; Crepel & Penit-Soria, 1986; Baker, Bostock, Grafe & Martius, 1987; Spain *et al.* 1987; Bobker & Williams, 1989; Eng *et al.* 1990). In general, two different types of hyperpolarization-activated inward currents have been distinguished. One is carried by K^+ ions, is blocked by Ba^{2+} and Cs^+ ions, has fast activation kinetics, and has an activation range which is dependent on the difference between membrane potential and potassium equilibrium potential (reviewed in Rudy, 1988). This hyperpolarization-activated K^+ current has traditionally been referred to as the inward rectifier. The other type is permeable to both Na^+ and K^+ ions, is selectively blocked by extracellular Cs^+ but not Ba^{2+}, has comparatively slow activation kinetics, and the activation range shows no dependence on the extracellular K^+ concentration (Halliwell & Adams, 1982; Mayer & Westbrook, 1983). The characteristics of the inward rectifier of thalamocortical relay cells resemble those of the Ba^{2+}-insensitive conductance in terms of ion selectivity, block by extracellular Cs^+ and activation kinetics. However, compared with the time- and voltage-dependent anomalous rectifier in hippocampal pyramidal cells (Halliwell & Adams, 1982), cerebellar Purkinje cells (Crepel & Penit-Soria, 1986), and cerebral cortical pyramidal cells (Spain *et al.* 1987) the corresponding current in thalamic neurones (I_h) appears to possess the distinctive feature of a much slower time course of activation which depends strongly on voltage. These characteristics make the inward rectifier in thalamic neurones similar to inwardly rectifying conductances found in sensory and sympathetic ganglion cells (Mayer & Westbrook, 1983; Tokimasa & Akasu, 1990) and heart cells (DiFrancesco, 1985). The differences in time course of activation suggest that there may exist more than one type of hyperpolarization-activated, time-dependent cation current in neurones. These differences may reflect either the existence of molecularly distinct subclasses of ionic channels or they may result from post-translational modifications of one common type of ionic channel, although available data cannot distinguish between these and other possibilities.

Functional role of I_h

The exact role of I_h in the complicated electrophysiological behaviour of thalamic neurones *in vivo* is not yet known. However, comparing the results obtained from recent intracellular recordings of the activity of thalamic neurones during different

neuronal states *in vivo* (reviewed by Steriade & Deschênes, 1984; Steriade & Llinás, 1988) with the physiological characteristics of I_h reported here suggests some strong possibilities.

Contribution of I_h to the resting membrane potential

An important function of I_h in thalamic neurones is the contribution to the normal resting potential. The value of the membrane potential critically determines the excitability and pattern of action potentials which are generated by thalamocortical relay neurones (Fig. 14; Jahnsen & Llinás, 1984*a*, *b*). Patterns of activity range from spontaneous single-spike firing at membrane potentials positive to −55 mV (Fig. 14*C*) to the rhythmic generation of burst discharges at more hyperpolarized levels (Fig. 14*B*). The normal resting potential of non-oscillating thalamic neurones of −60 to −70 mV is substantially positive to the presumed potassium equilibrium potential (−105 mV, McCormick & Prince, 1987), indicating that depolarizing currents contribute substantially to determining the membrane potential, even in the absence of synaptic inputs. A significant contribution of the inward current I_h to the resting potential is indicated by the hyperpolarization of the membrane from rest during extracellular application of Cs^+. This hyperpolarization was in general large enough to move the cell into the burst mode of action potential generation (Fig. 13*A*). Thus, recruitment of I_h in these cells can be assumed to move the membrane potential from a region where the low-threshold Ca^{2+} current is de-inactivated (i.e. able to be activated) into a region closer, but still subthreshold, to single-spike firing and in which the low-threshold Ca^{2+} current is inactivated. Thus I_h may contribute to establishing a true 'resting' condition between burst activity and generation of single spikes. In addition, the voltage sensitivity of I_h and the transient potassium currents which are activated by depolarization (D. A. McCormick, unpublished observations) serve to stabilize the membrane potential by compensating for either depolarizing or hyperpolarizing influences. Depending on the functional state of the brain, stronger inputs can move the membrane potential out of the indifferent region into a region of repetitive single-spike firing that would allow faithful transmission of incoming synaptic information or into a region of rhythmic burst discharges (reviewed in Steriade & Llinás, 1988).

Contribution of I_h to intrinsic thalamic oscillation

During certain periods of sleep, or under the influence of barbiturate anaesthesia, thalamic neurones generate high-frequency (300–500 Hz) bursts of two to six action potentials (McCarley, Benoit & Barrionuevo, 1983; Steriade & Deschênes, 1984). These high-frequency bursts may occur in a rhythmic or non-rhythmic manner. The two main types of rhythmic activity which have been observed *in vivo* are spindle waves and 1–2 Hz rhythmic bursting (Lamarre, Filion & Cordeau, 1971; Steriade & Deschênes, 1984; Steriade, Deschênes, Domich & Mulle, 1985). Spindle waves appear as an 8–12 Hz oscillation in the electroencephalogram and local thalamic field potential which steadily increases and then decreases in amplitude over approximately a 2 s period (Steriade & Deschênes, 1984). Spindle waves appear to be generated entirely within the thalamus and arise from the interaction of the GABAergic neurones of the thalamic reticular nucleus amongst themselves and

with thalamocortical relay neurones. Intracellular recordings from thalamocortical relay neurones *in vivo* during spindle waves indicate that this activity results from the periodic occurrence of low-threshold Ca^{2+} spikes activated by the offset of rhythmically occurring IPSPs which presumably are induced by burst discharges occurring in the inhibitory neurones of the thalamic reticular nucleus (Steriade & Deschênes, 1984).

In contrast to spindle wave generation, slow rhythmic (1–2 Hz) burst firing appears to be an endogenous property of cat thalamocortical relay neurones (Haby *et al.* 1988; McCormick & Prince, 1988). This type of rhythmic activity has been reported to occur in some stages of sleep (Lamarre *et al.* 1971) and is markedly enhanced by isolation of thalamocortical relay nuclei either through surgical knife cuts *in vivo* (Steriade *et al.* 1985) or through the maintenance of thalamic slices *in vitro* (McCormick & Prince, 1988).

In both types of rhythmic activity, the membrane potential of thalamic relay neurones oscillates within the activation range of I_h (e.g. between -60 and -85 mV), although the contribution of I_h to these two types of activity is likely to be somewhat different. The slow 1–2 Hz oscillation appears to depend critically upon the presence and strength of I_h (Figs 11–13). I_h may contribute to slow rhythmic burst firing in three distinct ways: (1) by causing an after-hyperpolarization following the generation of a burst; (2) by determining the overall range of membrane potential within which the neurone oscillates; and (3) by affecting the input conductance of the cell and therefore determining the responsiveness of the membrane potential to fluctuations in current flow.

The properties of the after-hyperpolarization which occurs after a depolarization or after the generation of a burst indicate that I_h contributes substantially to this physiological feature of thalamic neurones (Figs 12 and 13). The AHP occurs in a voltage range which is widely overlapping with the activation range of I_h, it can be elicited by largely passive depolarizations, its amplitude increases with increases in duration of the depolarization, and it is readily and reversibly blocked by Cs^+. In other neuronal systems, an AHP which is similar in time course is associated with the activation of a Ca^{2+}-activated potassium current, I_{AHP} (Pennefather, Lancaster, Adams & Nicoll, 1985; Lancaster & Adams, 1986). However, this current appears to be small or absent in LGND relay neurones (D. A. McCormick, unpublished observations).

The interaction of I_h and the low-voltage-activated Ca^{2+} current, I_t, appears to determine the 1–2 Hz rhythmic activity that is intrinsic to thalamocortical relay neurones (Fig. 14). The occurrence of a low-threshold Ca^{2+} spike is associated with de-activation of I_h. As the Ca^{2+} spike declines, due to inactivation of I_t, the lessened depolarizing influence of I_h creates a hyperpolarizing overshoot (the initial phase of the slow AHP). This hyperpolarization subsequently results in two important effects: removal of inactivation of I_t and activation of I_h (Fig. 14*B*). Activation of I_h depolarizes the membrane potential towards the threshold for activation of I_t and subsequently promotes the generation of a low-threshold Ca^{2+} spike. The generation of an additional Ca^{2+} spike results in the activation of a burst of fast Na^+–K^+-mediated action potentials, and so the cycle begins again.

Although the voltage-dependent properties of I_h and I_t, the behaviour of the AHP,

and the potent blocking ability of Cs^+, are all consistent with the proposed ionic substrate of slow rhythmic bursting, some additional points require further investigation. First, the rate of I_h de-activation (Fig. 3) appears slow compared with the duration of the Ca^{2+} spike (typically between 150 and 200 ms). However, one must take into account the strong voltage dependence of the rate of I_h de-activation (Fig. 3). For example, the time constant of I_h de-activation averages 347 ms at -55 mV, the most positive voltage at which it could be determined. During a typical Ca^{2+} spike, that is elicited from about -80 mV, the membrane depolarizes to between -50 and -40 mV. The resulting reduction of the time constant of I_h de-activation might allow a large portion of I_h to de-activate during the Ca^{2+} spike. In addition, the hyperpolarization-activated cation current, I_f, in sino-atrial cells of the heart has recently been shown to be strongly sensitive to the concentration of intracellular Ca^{2+} (Hagiwara & Irisawa, 1989). Assuming a similar sensitivity of I_h to $[Ca^{2+}]_i$, the occurrence of low-threshold Ca^{2+} spikes in thalamic neurones may enhance de-activation of I_h during depolarization and activation upon hyperpolarization, thereby increasing the amplitude of the after-hyperpolarization.

An additional point of consideration is that other voltage-dependent conductances might contribute to the 1–2 Hz rhythmic firing in thalamic neurones. For example, cardiac pacemaking, which is based to a large degree on the properties of a similar, hyperpolarization-activated cation current, I_f (reviewed by DiFrancesco, 1985, and Noble, 1985), is also strongly influenced by other ionic currents, such as a slow inward current (I_{SI}) and the delayed rectifier current (I_K) (see review by DiFrancesco & Noble, 1989). In thalamic neurones, the 'classical' delayed rectifier does not seem to contribute to the generation of rhythmic activity, since its activation threshold is not reached by the Ca^{2+} spike. However, the transient voltage-dependent potassium currents, I_A or I_D (Jahnsen & Llinás, 1984*a*, *b*; Storm, 1988), have voltage ranges of activation and inactivation which are largely overlapping with I_t (D. A. McCormick & H.-C. Pape, unpublished observations) and therefore may slow the approach to threshold for the Ca^{2+} spike. In addition, the persistent Na^+ inward current (Jahnsen & Llinás, 1984*a*, *b*) could play a similar role to that demonstrated for the slow inward current in cardiac Purkinje cells. In conclusion, the present data reveal a critical role of I_h in slow thalamic oscillations. The possible influences of other ionic conductances, or ionic pumps, however, remain to be investigated in detail (e.g. see review by Noble *et al.* 1989).

The influence of I_h on spindle oscillations will differ to some extent from that on slow rhythmic burst firing due to the fact that spindle wave generation in relay cells relies upon the occurrence of rhythmic barrages of IPSPs (Steriade & Deschênes, 1984). The time- and voltage-dependent activation of I_h may contribute to spindle oscillations by influencing the amplitude and time course of these IPSPs. The amplitude of these IPSPs will be determined in part by the resting membrane conductance, which can be strongly influenced by I_h. Thus, increases in activation of I_h may be capable of decreasing the responsiveness of thalamocortical relay neurones to IPSPs (see McCormick & Pape, 1990). In addition, the activation of I_h by the hyperpolarization associated with IPSPs, particularly those mediated by increases in potassium conductance (Hirsch & Burnod, 1987; Crunelli, Haby, Jassik-Gerschenfeld, Leresche & Pirchio, 1988), will contribute to a faster repolarization

of the membrane, particularly during the repolarizing phase of the IPSP. This, in turn, may strongly influence the pattern of activity generated in response to these synaptic inputs.

In conclusion, activation and de-activation of I_h has important functional consequences in controlling the responsiveness of thalamic neurones to transient or sustained hyperpolarizations, in providing the pacemaking for slow oscillatory burst activity, and in contributing to the determination of the membrane potential during different states of neuronal function.

We thank Hilarey Feeser and Anne Williamson for critical comments on this manuscript. This research was funded by the National Institute of Health, the Klingenstein Fund, and the Jacobs Javits Center in Neuroscience (D.A.M.), and the Deutsche Forschungsgemeinschaft (Ey 8/14-1; Ey 8/17-1) and the Minister für Wissenschaft und Forschung NRW (401 452 89) (H.-C.P.).

REFERENCES

ALONSO, A. & LLINÁS, R. R. (1989). Subthreshold Na^+-dependent theta-like rhythmicity in stellate cells of entorhinal cortex layer II. *Nature* **342**, 175–177.

BAKER, M., BOSTOCK, H., GRAFE, P. & MARTIUS, P. (1987). Function and distribution of three types of rectifying channel in rat spinal root myelinated axons. *Journal of Physiology* **383**, 45–67.

BOBKER, D. H. & WILLIAMS, J. T. (1989). Serotonin augments the cation current I_h in central neurons. *Neuron* **2**, 1535–1540.

COULTER, D. A., HUGUENARD, J. R. & PRINCE, D. A. (1989). Calcium currents in rat thalamocortical relay neurones: kinetic properties of the transient, low-threshold current. *Journal of Physiology* **414**, 587–604.

CREPEL, F. & PENIT-SORIA, J. (1986). Inward rectification and low threshold calcium conductance in rat cerebellar Purkinje cells. An *in vitro* study. *Journal of Physiology* **372**, 1–23.

CRUNELLI, V., HABY, M., JASSIK-GERSCHENFELD, D., LERESCHE, N. & PIRCHIO, M. (1988). Cl^-- and K^+-dependent inhibitory postsynaptic potentials evoked by interneurones of the rat lateral geniculate nucleus. *Journal of Physiology* **399**, 153–176.

CRUNELLI, V., KELLY, J. S., LERESCHE, N. & PIRCHIO, M. (1987*a*). The ventral and dorsal lateral geniculate nucleus of the rat: intracellular recordings *in vitro*. *Journal of Physiology* **384**, 587–601.

CRUNELLI, V., LERESCHE, N., HYND, J. E., PATEL, N. M. & PARNAVELAS, J. G. (1987*b*). An in vitro slice preparation of the cat lateral geniculate nucleus. *Journal of Neuroscience Methods* **20**, 211–219.

CRUNELLI, V., LIGHTOWLER, S. & POLLARD, C. E. (1989). A T-type Ca^{2+} current underlies low-threshold Ca^{2+} potentials in cells of the cat and rat lateral geniculate nucleus. *Journal of Physiology* **413**, 543–561.

DIFRANCESCO, D. (1985). The cardiac hyperpolarizing-activated current, I_f, origins and developments. *Progress in Biophysics and Molecular Biology* **46**, 163–183.

DIFRANCESCO, D. & NOBLE, D. (1989). Current I_f and its contribution to cardiac pacemaking. In *Neuronal and Cellular Oscillators*, ed. JACKLETT, J. W., pp. 31–57. M. Dekker, Inc., New York.

ENG, D. L., GORDON, T. R., KOCSIS, J. D. & WAXMAN, S. G. (1990). Current clamp analysis of a time-dependent rectification in rat optic nerve. *Journal of Physiology* **421**, 185–202.

HABY, M., LERESCHE, N., JASSIK-GERSCHENFELD, D., SOLTESZ, I. & CRUNELLI, V. (1988). Spontaneous rhythmic depolarization in the principal cells of the lateral geniculate body in vitro: the role of NMDA receptors. *Compte rendus hebdomadaire des séances de l'Académie des sciences, Series III* **306**, 195–199.

HAGIWARA, N. & IRISAWA, H. (1989). Modulation by intracellular Ca^{2+} of the hyperpolarization-activated inward current in rabbit single sino-atrial node cells. *Journal of Physiology* **409**, 121–141.

HALLIWELL, J. V. & ADAMS, P. R. (1982). Voltage-clamp analysis of muscarinic excitation in hippocampal neurons. *Brain Research* **250**, 71–92.

HERNÁNDEZ-CRUZ, A. & PAPE, H.-C. (1989). Identification of two calcium currents in acutely dissociated neurons from the rat lateral geniculate nucleus. *Journal of Neurophysiology* **61**, 1270–1283.

HIRSCH, J. C. & BURNOD, Y. (1987). A synaptically evoked late hyerpolarization in the rat dorsal lateral geniculate nucleus in vitro. *Neuroscience* **23**, 457–468.

HIRSCH, J. C., FOURMENT, A. & MARC, M. E. (1983). Sleep-related variations of membrane potential in the lateral geniculate body relay neurons of the cat. *Brain Research* **259**, 308–312.

HOTSON, J. R., PRINCE, D. A. & SCHWARTZKROIN, P. A. (1979). Anomalous inward rectification in hippocampal neurons. *Journal of Neurophysiology* **42**, 889–895.

ISHIHARA, K., MITSUIYE, T., NOMA, A. & TAKANO, M. (1989). The Mg^{2+} block and intrinsic gating underlying inward rectification of the K^+ current in guinea-pig cardiac myocytes. *Journal of Physiology* **419**, 297–320.

JAHNSEN, H. & LLINÁS, R. (1984*a*). Electrophysiological properties of guinea-pig thalamic neurones: an *in vitro* study. *Journal of Physiology* **349**, 105–226.

JAHNSEN, H. & LLINÁS, R. (1984*b*). Ionic basis for the electroresponsiveness and oscillatory properties of guinea-pig thalamic neurones *in vitro*. *Journal of Physiology* **349**, 227–247.

LAMARRE, Y., FILION, M. & CORDEAU, J. P. (1971). Neuronal discharge of the ventrolateral nucleus of the thalamus during sleep and wakefulness in the cat. I. Spontaneous activity. *Experimental Brain Research* **12**, 480–498.

LANCASTER, B. & ADAMS, P. R. (1986). Calcium-dependent current generating the afterhyperpolarization in hippocampal neurons. *Journal of Neurophysiology* **55**, 1268–1282.

LIGHTOWLER, S., HYND, J. W., POLLARD, C. E. & CRUNELLI, V. (1989). Inward rectification of projection cells in the rat and cat lateral geniculate nucleus. *Society for Neuroscience Abstracts* **15**, 1310.

LIVINGSTONE, M. S. & HUBEL, D. H. (1981). Effects of sleep and arousal on the processing of visual information in the cat. *Nature* **291**, 554–561.

MCCARLEY, R. W., BENOIT, O. & BARRIONUEVO, G. (1983). Lateral geniculate nucleus unitary discharge in sleep and waking: State- and rate-specific aspects. *Journal of Neurophysiology* **50**, 798–818.

MCCORMICK, D. A. & PAPE, H.-C. (1988). Acetylcholine inhibits identified interneurons in the cat lateral geniculate nucleus. *Nature* **334**, 246–248.

MCCORMICK, D. A. & PAPE, H.-C. (1990). Noradrenergic and serotonergic modulation of a hyperpolarization-activated cation current in thalamic relay neurones. *Journal of Physiology* **431**, 319–342.

MCCORMICK, D. A. & PRINCE, D. A. (1987). Actions of acetylcholine in the guinea-pig and cat medial and lateral geniculate nuclei, *in vitro*. *Journal of Physiology* **392**, 147–165.

MCCORMICK, D. A. & PRINCE, D. A. (1988). Noradrenergic modulation of firing pattern in guinea pig and cat thalamic neurons, in vitro. *Journal of Neurophysiology* **59**, 978–996.

MATSUDA, H., SAIGUSA, A. & IRISAWA, H. (1987). Ohmic conductance through the inwardly rectifying K channel and blocking by internal Mg^{2+}. *Nature* **325**, 156–159.

MAYER, M. L. & WESTBROOK, G. L. (1983). A voltage-clamp analysis of inward (anomalous) rectification in mouse spinal sensory ganglion neurones. *Journal of Physiology* **340**, 19–45.

NOBLE, D. (1985). Ionic mechanisms in rhythmic firing of heart and nerve. *Trends in Neurosciences* **8**, 499–504.

NOBLE, D., DIFRANCESCO, D. & DENYER, J. (1989). Ionic mechanisms in normal and abnormal cardiac pacemaker activity. In *Neuronal and Cellular Oscillators*, ed. JACKLETT, J. W., pp. 59–85. M. Dekker, Inc., New York.

PENNEFATHER, P., LANCASTER, B., ADAMS, P. R. & NICOLL, R. A. (1985). Two distinct Ca-dependent K currents in bullfrog sympathetic ganglion cells. *Proceedings of the National Academy of Sciences of the USA* **82**, 3040–3044.

RUDY, B. (1988). Diversity and ubiquity of K channels. *Neuroscience* **25**, 729–749.

SPAIN, W. J., SCHWINDT, P. C. & CRILL, W. E. (1987). Anomalous rectification in neurons from cat sensorimotor cortex in vitro. *Journal of Neurophysiology* **57**, 1555–1576.

STERIADE, M. & DESCHÊNES, M. (1984). The thalamus as a neuronal oscillator. *Brain Research Reviews* **8**, 1–63.

STERIADE, M., DESCHÊNES, M., DOMICH, L. & MULLE, C. (1985). Abolition of spindle oscillations in thalamic neurons disconnected from nucleus reticularis thalami. *Journal of Neurophysiology* **54**, 1473–1497.

STERIADE, M. & LLINÁS, R. (1988). The functional states of the thalamus and the associated neuronal interplay. *Physiological Reviews* **68**, 649–742.

STORM, J. F. (1988). Temporal integration by a slowly inactivating K^+ current in hippocampal neurons. *Nature* **336**, 379–381.

TOKIMASA, T. & AKASU, T. (1990). Cyclic AMP regulates an inward rectifying sodium–potassium current in dissociated bull-frog sympathetic neurones. *Journal of Physiology* **420**, 409–429.

YANAGIHARA, K. & IRISAWA, H. (1980). Inward current activated during hyperpolarization in the rabbit sino atrial node cell. *Pflügers Archiv* **385**, 11–19.